Magnetic Emission Technique in Assessing Dynamic Fracture Mechanics Parameters of Ductile Steel

Zoran Radaković

Teaching and Research Assistant

University of Belgrade
Faculty of Mechanical Engineering

Concerning new challenges in structural integrity assessment, the identification of relaxation and service life extension of structural steels by qualitative and quantitative determination of dynamic fracture mechanics parameters is highly significant. Problems in experimental research are in connection with precise determination of resistance to fracture in conditions of dynamic loading of structures, where standard procedures in the case of precracked Charpy specimens are yet to be defined.

Instrumented Charpy testing is performed by magnetic emission (ME) technique for determining critical crack initiation properties in a steel of dominant ductile properties. The equivalent brittle, ductile, and mixed fracture behaviour is simulated by the choice of test temperature and impact velocity. Analysis of acquired ME and integrated ME signals, both employed in deriving the critical J integral, has been successful in interpreting the results for unstable or stable crack propagation.

Keywords: *dynamic fracture mechanics, impact testing, fracture toughness, ductility, ferritic steel, magnetic emission, crack initiation, crack propagation.*

1. INTRODUCTION

Steel structures made of structural low-alloyed steel usually undergo cleavage fracture when ambient temperatures fall below nil ductility temperature. Certain microalloyed steel compositions may prevent this, particularly if they retain high ductility at lower temperatures. The dynamic mode of loading is more critical for a structure than the static, and determination of dynamic fracture mechanics properties of structural steels is necessary. Various types of fracture are evident from force-time records of instrumented impact tests. A high strength low alloyed steel (HSLA) is tested by applying dynamic loads at very–low, low, and room temperatures so that all three regions of characteristic temperature behaviour are included (ductile, mixed, and brittle). The nil ductility temperature range for most HSLA steels is between –50°C and –70°C. Impact rates are defined by choosing potential energy levels of 300 J and 62,5 J, enabling impact loading rates $v_o = 5,5$ and $2,6$ m/s, in respect. The fatigue cracks produced on standard Charpy specimens that also influence the fracture toughness are inside the range: $a/W = 0,47...0,57$, enabling the assessment of dynamic fracture mechanics parameters.

One of the most widely used techniques for this purpose is the instrumented impact test. In this case the instrumentation consists of magnetic emission (ME) technique (Winkler, 1988; Winkler 1990; Lenkey and Winkler, 1997; Lenkey 1997). This technique is used to determine crack initiation and propagation in brittle and ductile steels under dynamic loading.

Unstable crack initiation, usually evident in brittle fracture, is directly indicated by the ME signal. Stable crack initiation, in case of ductile or mixed mode fracture, is usually difficult to identify from the ME signal, so instead, it may be depicted from the characteristic change in the integrated ME signal (sometimes designated by MF, as it is proportional to the magnetic field). The ME signal is integrated in the time domain and early results have been compared to conventional R– curve and stretch zone assessment methods (Lenkey and Winkler, 1997).

The most useful specific parameter in calculating the critical data is the crack initiation time, t_i. Failure in the case of ductile material behaviour may be expressed by both stable and unstable crack propagation. This paper shows examples of numerous tests carried out on the same material, showing varying indications of crack initiation time, or time-to-fracture (t_F), intentionally caused by directing the material behaviour from brittle to ductile and vice versa, all in the scope of searching for objectives based on this experience.

2. THEORETICAL FRAMEWORK

In general, ferritic steels have the characteristic fracture toughness change with temperature as depicted in Fig. 1 (Rintamaa, 1996; Lenkey, 1997).

The lower shelf region (I) is characterised by cleavage fracture, while the upper shelf region (III) by ductile dimple fracture mechanism. Region (II) is a mixed

mode fracture, where both cleavage and ductile fracturing mechanisms may occur. The lack of dynamic testing standards for pre-cracked Charpy specimens has demanded the use of standard linear elastic fracture mechanics quasi-static tests (ASTM E 399), or elastic-plastic fracture mechanics tests (ASTM E 813), intended for determining the critical stress intensity factor, K_{Ic}, and the J integral, respectively.

Depending on the fracture behaviour of the specimen, different *load–time* responses are observed, Fig. 2. The initial oscillations in the loading signal, at the start of impact, originate from mechanical oscillations in the *specimen–striker* system. If these oscillations should fall substantially to the value of the characteristic load used in calculations, the loading process may be treated as quasi-static. This condition is formulated according to "3τ"criterion (Kalthoff, 1985), which states that at least 3 oscillations must precede the fracture of specimen. If this criterion is fulfilled, the derived expressions for static fracture mechanics testing conditions may be applied for determining dynamic fracture mechanics parameters, according to original ASTM standards (ASTM E-399; ASTM E 813-89), and their newer combinations (ASTM E 1152; ASTM E 1737; ASTM E 1820–01).

In case of linear elastic behaviour (the curve to point B in Fig. 2, and also regions I and II in Fig. 1), the dynamic fracture toughness, K_{Id}, may be determined in a similar way as in static tests, but under the condition that the "3τ"criterion is fulfilled. The parameter is calculated from eqn. (1), where the characteristic load is the force at the moment of unstable crack initiation, F_1 (e.g. at instances B, C, and D on Fig. 2), and for geometry conditions, $L/W = 4$,

$$K_{Id} = \frac{F_1}{BW^{1/2}} Y\left(\frac{a_o}{W}\right) \qquad (1)$$

where: L (mm)–anvil span; F_1 (N)–force at the onset of unstable crack initiation (only for case B in Fig. 2); B (mm)–specimen thickness; W (mm)–specimen width; a_o (mm)–initial crack length; $Y(a_o/W)$–geometry constant.
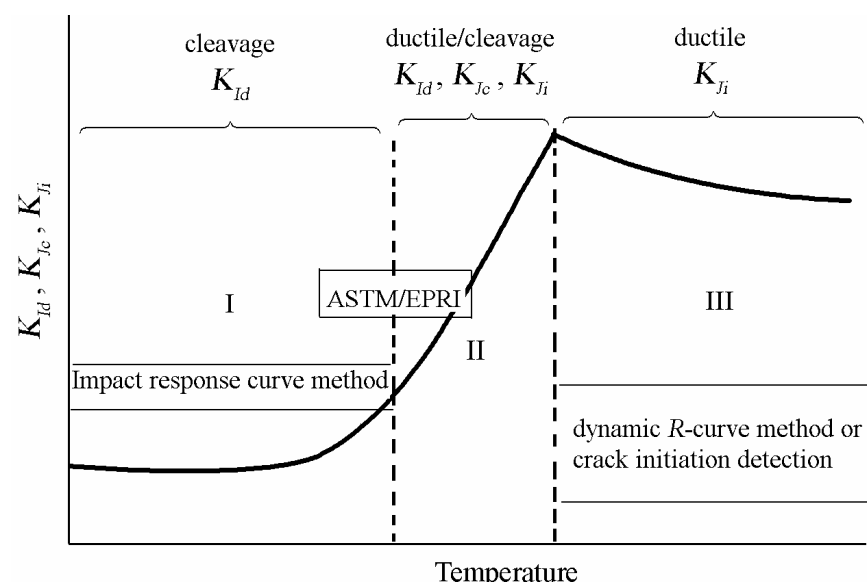

Figure 1. The ductile-brittle fracture toughness transition curve with ranges of application: I–impact response curves (Kalthoff, 1985); II–ASTM/EPRI procedure, (Ireland, 1980; Server et al., 1975); and III with newer methods as dynamic *R*-curve or the ductile crack initiation detection.
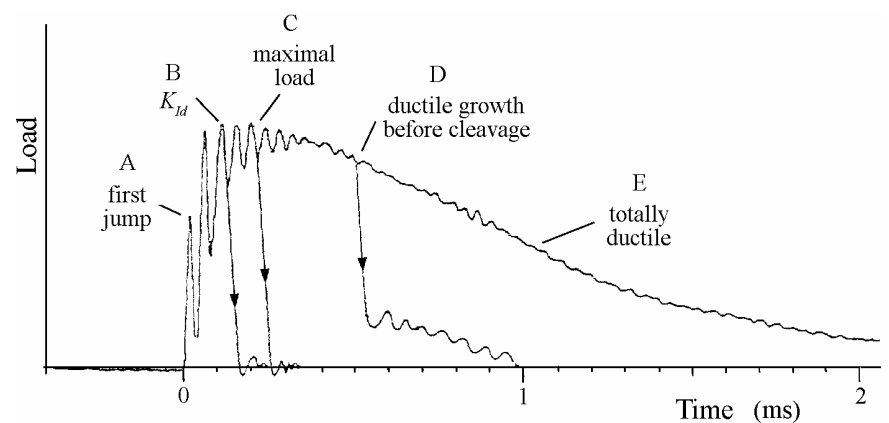

Figure 2. Typical *load-time* diagram from dynamic instrumented testing.

When conditions for the "3τ"criterion are not fulfilled, the *impact response curve concept* may be applied for determining K_{Id} (Kalthoff, 1985). This procedure does not require load instrumentation, but only instrumentation necessary for measuring *time–to–fracture*, (Kalthoff, Winkler, 1983). A few methods satisfy this requirement, e.g. specimens instrumented with strain gauges, or, by magnetic emission technique. Measured time–to–fracture, t_F, enables determination of fracture toughness according to the relationship

$$K_{Id} = Rv_o t'' \qquad (2)$$

where: v_o–impact speed; $t'' = f(t')$, $t' = g(t)$–modified time parameters, t–measured physical time, f and g–functions account for dynamic corrections and variations of crack length, respectively; $R = 301k$ GN/m$^{5/2}$ with the first-order correction factor $k = 1{,}276/(1+0{,}276C_M/8{,}1\times10^{-9}$ m/N) (Kalthoff, 1985). Accounting for test device stiffness and machine compliance, $C_M = 2{,}335\times10^{-8}$ m/N, the correction factor is calculated, $k = 0{,}711$.

In case of *linear elastic–plastic* behaviour with considerable plastic deformation, and possibility of stable crack growth preceding unstable growth (position C in Fig. 2 and region II in Fig. 1), the J integral value for unstable crack initiation represents the material fracture resistance characteristic. According to the original ASTM Standard E 813-89 (1996), this parameter may be evaluated from the *load–displacement* curve in the following way

$$J_{Id} = J_{el} + J_{pl} \qquad (3)$$

where J_{el} and J_{pl} are the elastic and plastic component of J, in respect, and are evaluated from

$$J_{el} = \frac{K_{cd}^2 \left(1 - \nu^2\right)}{E} \text{ (for plane strain)} \qquad (4)$$

and

$$J_{pl} = \frac{2U_{pl}}{B\left(W - a_o\right)} \qquad (5)$$

where: U_{pl}–plastic work, evaluated from the surface area under the *load–displacement* curve, up to the onset of unstable fracture, or to the unloading point. In the upper relation, K_{cd} is the *critical dynamic* stress intensity factor at unstable crack initiation, due to critical load, F_1, and may be evaluated according to eqn. (1).

The load–displacement curve is determined by integrating twice the load–time curve. Striker speed changes according to

$$v(t) = v_o - \frac{1}{m} \int_{t=0}^{t} F(t)\, dt \qquad (6)$$

where: m (kg), is the striker mass; v_o (m/s)–impact speed; $F(t)$ (N)–function of load vs. time.

The displacement–time function is calculated from

$$s(t) = \int_{t=0}^{t} v(t)\, dt \qquad (7)$$

The third special case occurs at completely stable crack growth, or when crack development is mostly stable (shown by examples of behaviour E and D, respectively, on the load–time diagram, Fig. 2, and by region III–ductile type behaviour, Fig. 1). In this particular case, material behaviour can be characterised by the critical J integral value at the onset of ductile crack initiation, usually interpreted in two different ways: by critical J integral at initiation of crack growth; or from the J integral value at stable crack extension, $\Delta a = 0{,}2$ mm, derived by the dynamic resistance curve, or R-curve method.

3. MATERIAL AND EXPERIMENTS

The tested material is a high strength steel in normalised condition, treated by mechanical hot controlled rolling and rapidly cooled, produced by US Steel Serbia, Smederevo, 1995. It is delivered in the shape of 12 mm thick plates, contains 0,075% C, and is microalloyed with Nb and Ti. Yield strength is $\sigma_y = 411$ MPa. The tested steel is very ductile at low temperatures, with a temperature transition region from –40°C to –60°C.

Charpy V specimens were cut, with notch radius $r = 0{,}25...0{,}3$ mm. The specimen geometry and sizes are shown altogether with two selected orientations, a total of 78 specimens of the L–S, and 63 specimens of the T–S orientation were tested (see Figs. 3 and 4).
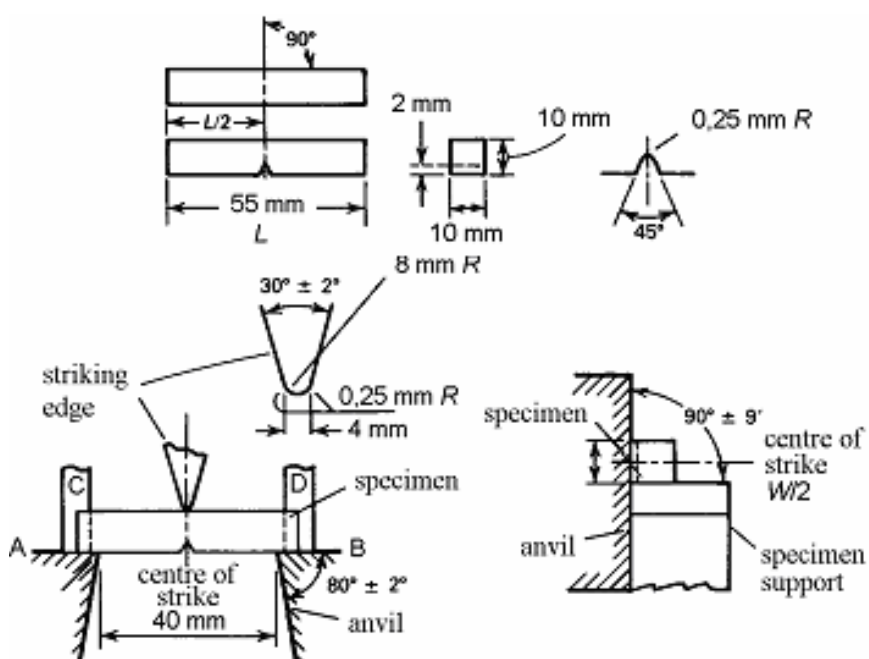

Figure 3. Standard Charpy V-notch specimens and the striker-anvil arrangement (according to ASTM E-399).

All specimens were pre-cracked by high cycle fatigue according to a previously generated fatigue programme that ensured no visible plastic strains around the crack

tip and length/width ratios within limits $a/W = 0{,}35...0{,}65$. These values are equally distributed around the standard fracture mechanics value of 0,5. Specimens are divided into three groups: A (long pre-cracks, $a/W = 0{,}55...0{,}65$); B (intermediate, $a/W = 0{,}45...0{,}55$); and C (shorter pre-cracks, $a/W = 0{,}35...0{,}45$), (Radaković, 2004).
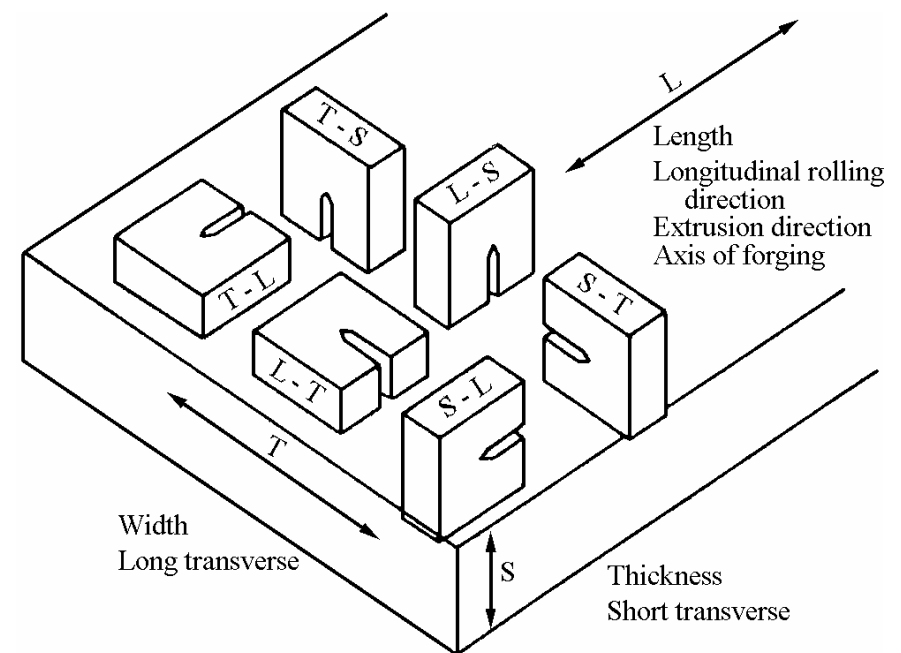

Figure 4. Notched specimen orientation in plated material.

3.1. Temperature and impact speed effects

Test conditions with varying temperature and impact speed dictate the behaviour of ductile steel as such that these parameters may often have an opposite effect. Figure 5 shows that the yield stress in dynamic tests may also decrease with the rise in strain rate (Lenkey, 2003). It is obvious that brittle material behaviour appears at conditions of higher loading rates and/or lower temperatures.
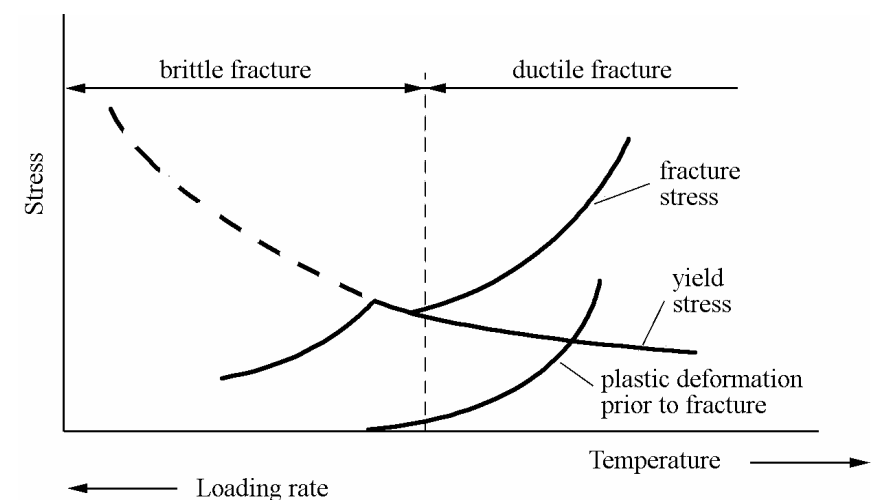

Figure 5. Effect of loading rate and temperature on the material behaviour in the impact test, (Lenkey, 2003).

Three characteristic temperatures are chosen for testing (–70°C, –30°C, and +20°C), since it is known that the HSLA steel is brittle at –70°C, and very ductile at +20°C, while at –30°C it has a mixed fracture behaviour, i.e. mixed ductile–brittle fracture mode in the transition region. The choice of temperatures enabled the requirement for at least three or more procedures in assessing the behaviour of the material, as if three materials with different modes fracture were tested instead of one.

The temperature influence on the energy for fracture in ferritic steels is closely connected to the acting microscopic mechanism of fracture: cleavage at lower– and

void coalescence at higher temperatures. The occurrence of cleavage and brittle behaviour in ferritic steels are closely connected (particularly in low strength steels), thus terms "cleavage" and "brittleness" have been frequently used as synonyms in literature. This is erroneous in the general case, because brittleness is defined at low *energy* levels of fracture, or by limited plasticity at the crack tip, while cleavage is used to describe the *micro-mechanism* for fracture. The confusion appears in many instances, since brittle behaviour may manifest without cleavage, as is the case of fracture in high strength aluminium alloys. In contrast, elongation of 4% (corresponding to mean absorption energy) can appear in specimens of W–Re alloys, which still fracture by cleavage. It is known that there is not always a direct connection between the given fracturing mechanism and the energy value for fracture, so these terms should be treated separately.

3.2. Charpy instrumentation

Recording of the load signals as a function of real time in the process of fracture is possible with the instrumented Charpy machine. The data acquisitioning and storing system forms the additional instrumentation in the magnetic emission system. The instrumentation scheme is shown in Fig. 6.

Loads (forces) are measured by strain gauges, glued on both sides of the striker (position 3, Fig. 6). The magnetic and electric emission probes (5) are located inside the striker box profile. The optical triggering device (6) activates the data acquisitioning system. Two optical signals are released at a time interval measured by the digital clock, and the true impact speed is calculated. The digital four-channel PC compatible oscilloscope (10) has a *T-trigger* and 200 Hz frequency capacity, making it possible to record up to 100 MS/s.

All recorded data are processed by spreadsheet analysis consisting of algorithms specifically incorporated for this matter (Radaković, 2004).
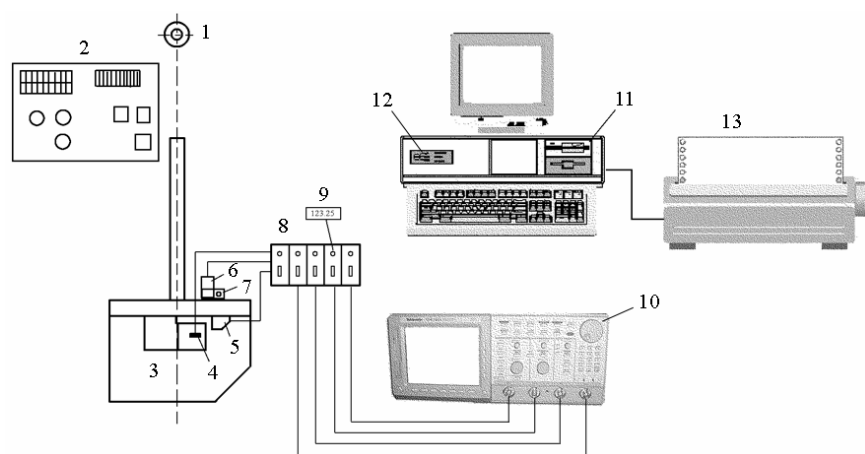
Figure 6. Charpy instrumentation scheme and data acquisitioning system. 1-angle measurement; 2-pendulum controls; 3-tup; 4-strain gauge; 5-magnetic probe; 6-trigger device; 7-triggering flags; 8-power supply and amplifiers; 9-LED clock; 10-oscilloscope; 11-PC; 12-GPIB interface; 13-printer

4. RESAULTS AND DISCUSION

An example of a *force–time–magnetic emission* (*F–t*–ME) and of a *force–time–integrated magnetic emission* (*F–t*–MF) diagram are shown in Figs. 7a, b for a single specimen tested at −70° with impact speed v_o = 5,5 m/s, and in Figs. 8a, b for a single specimen tested at

+20°C and v_o = 2,59 m/s. Both specimens are produced with similar pre-crack lengths of a_o = 4,27 mm and 4,44 mm, respectively.

The difference in the MF curves of the two tested specimens is noticeable. The MF curve of the second specimen, in Fig. 8b, spreads in a much wider time interval which results in longer time-to-fracture, t_F. Actually, this quantity is t_F = 90 μs and 160 μs, for the shown specimens U019 and U087, respectively. A later onset of ductile crack initiation is indicated in the latter specimen. This is an example of stable crack propagation initiating at 0.767 ms (Fig. 8b), while the case of brittle fracture is evident in the former specimen, where unstable crack propagation initiates at 0,364 ms (Fig. 7b).

As a rule, the *F–t*–MF diagram analyses require good knowledge of the studied magnetic phenomena in the ferro-magnetic material, whereas this might implicate complex fracture behaviour, sometimes changing from stable to unstable, and vice versa. Most often, analysis is required for both diagrams *F–t*–ME and *F–t*–MF, and for the force–time diagrams (*F–t*) as well.
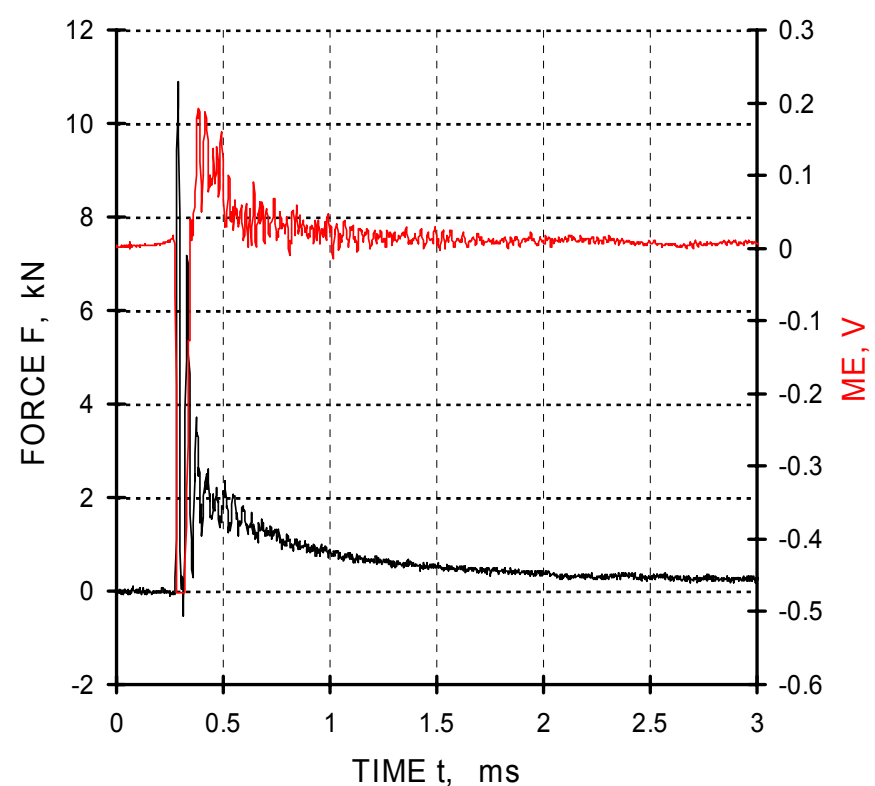
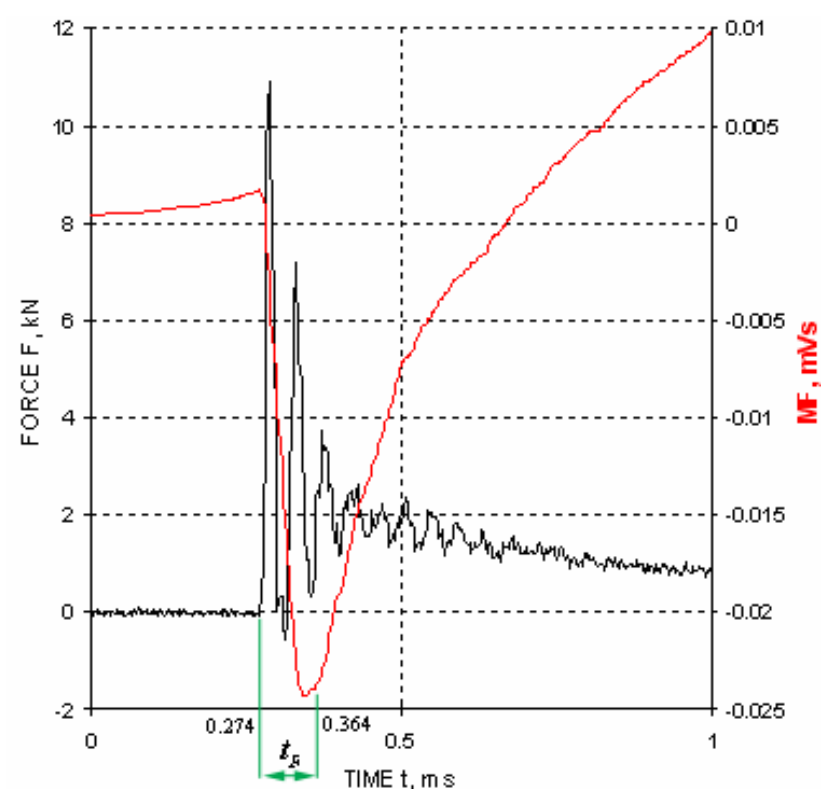**Figure 7a. Force–time–ME diagram, specimen U019 (E_o = 300 J, T = −70°C, and pre-crack a_o = 4,27 mm).**
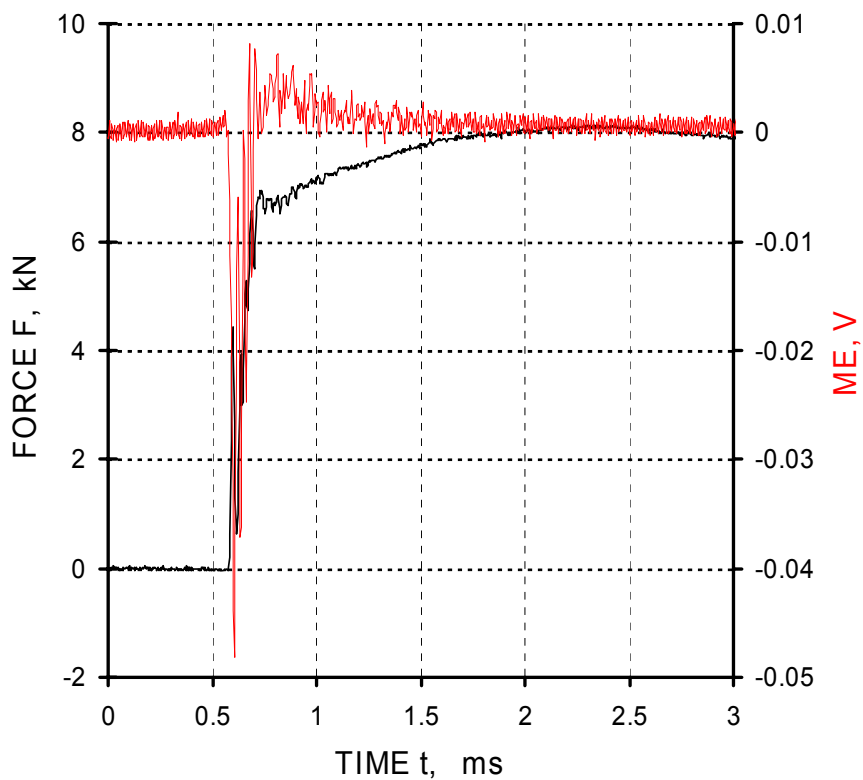
Figure 7b. Force–time–MF diagram (specimen U019).

Figure 8a. Force–time–ME diagram, specimen U087 (E_o = 62 J; T = +20°C; a_o = 4,44 mm).
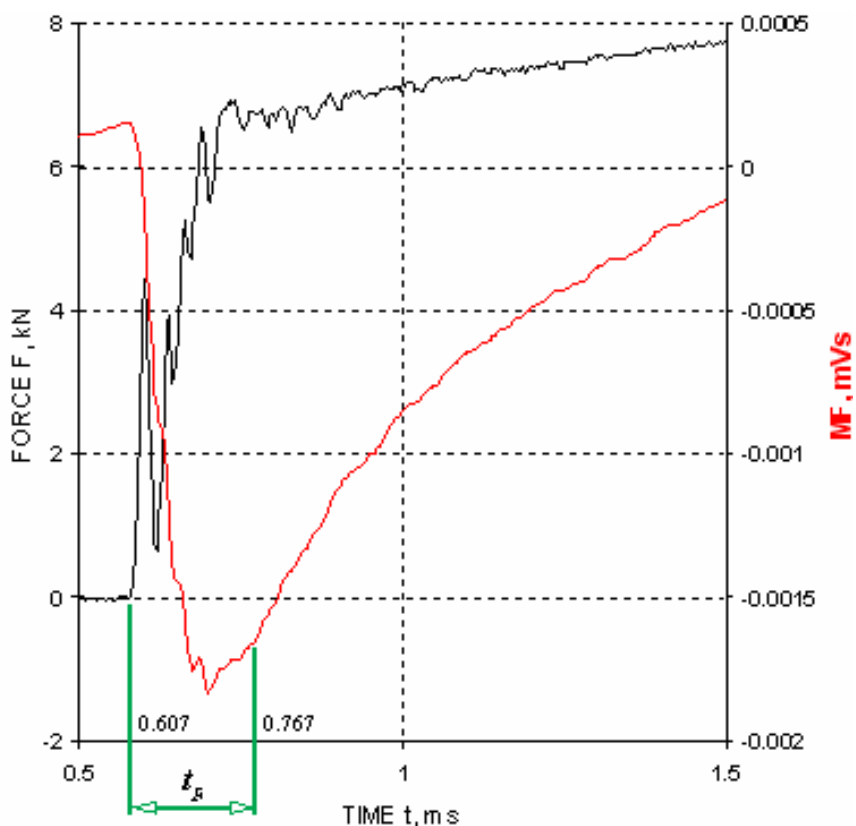

Figure 8b. Force–time–MF diagram (specimen U087).

The analysis of several hundred diagrams of the 141 tested specimens has led to some of the results shown in Figs. 9–12 that represent diagrams of characteristic dynamic fracture mechanics parameters: critical dynamic J integral evaluated from ME measurements (J_{cm}^{d}); dynamic fracture toughness for mode I (crack opening type) fracture (K_{Id}). This parameter is evaluated according to the response curve method (for low and intermediate temperatures). Parameter K_{Ji} is the critical stress intensity factor evaluated from the critical dynamic J_{cm}^{d} integral, according to ME measurements. The parameter K_{Jc} is the critical stress intensity factor derived from both elastic-plastic fracture mechanics analysis (Tada, Paris, Irwin, 1973) and ASTM/EPRI procedures.

The J integral parameters are shown as a function of initial pre-crack length, a_o, and specimen orientation. The fracture toughness, or critical stress intensity factor parameters are shown as a function of temperature, T, for both of the tested specimen orientations.

Figure 9 shows a mild indicated drop in the dynamic J integral with respect to pre-crack length, J_{cm}^{d}–a_o, for specimen orientations L–S and T–S (designated by U

and P). The curves for the two specimen orientations are very close and equidistant, with expected lower J integral values for the T–S orientation.
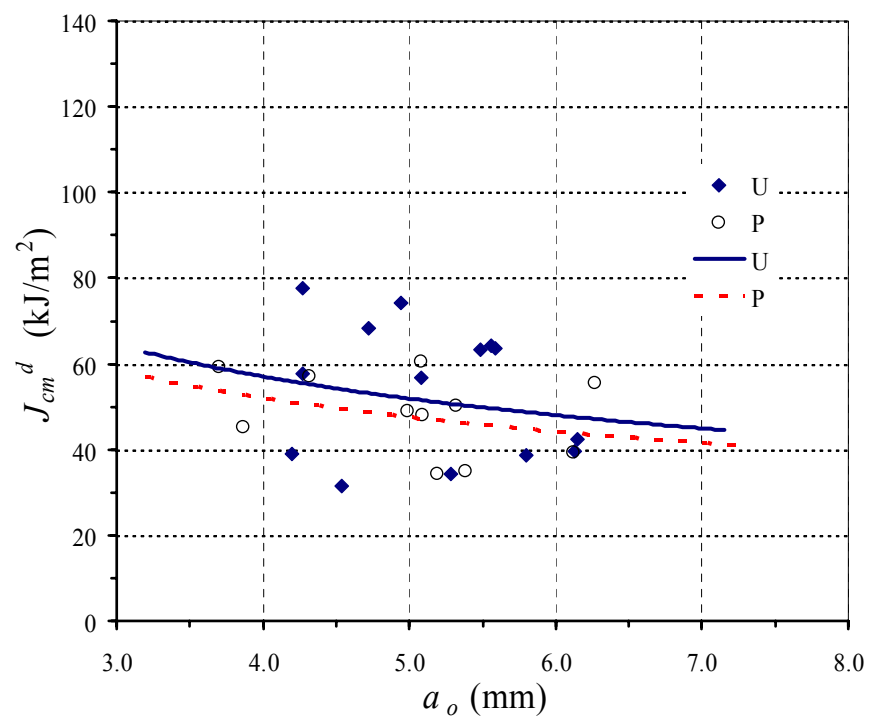

Figure 9. J integral vs. pre-crack length for specimen orientations U and P, (v_o = 5,5 m/s, E_o = 300 J, T = –70°C).

Figure 10 shows results of the J_{cm}^{d}–a_o dependence for both specimen orientations, where the testing conditions are totally different from those shown in Fig. 9. Compared to the prior case, the J integral value is lesser sensitive to pre-crack length because of lower impact speed, and the effect of specimen orientation is such that the curves U and P intersect, indicating very little or no influence of the texture orientation for longer pre-crack lengths.
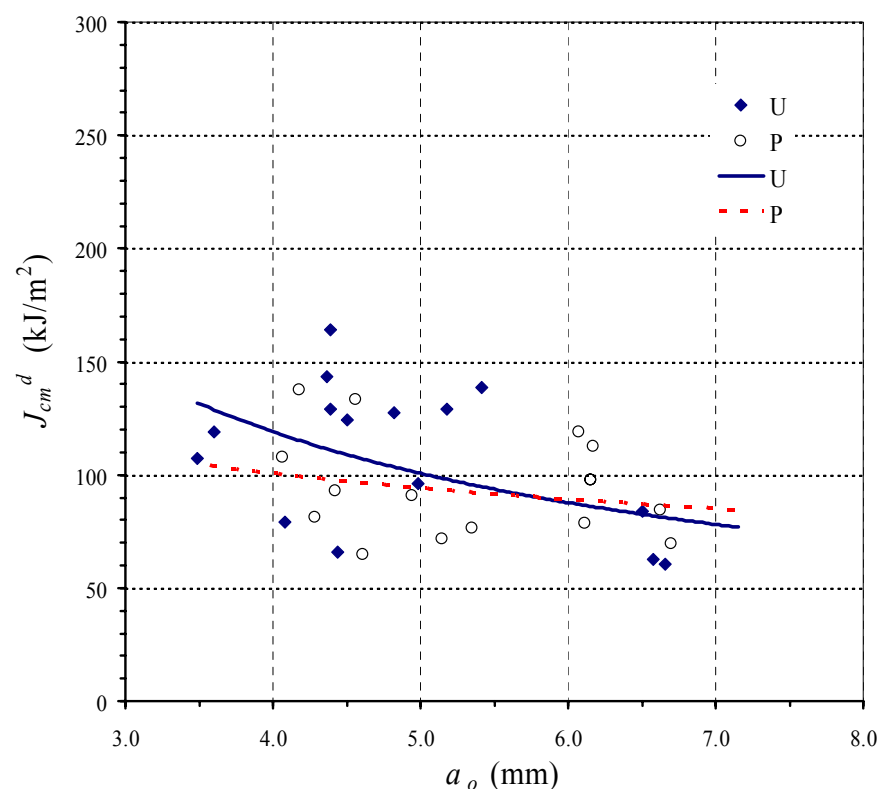

Figure 10. J_{cm}^{d}–a_o dependence for specimen orientations U and P, (v_o = 2,59 m/s, E_o = 62 J, T = +20°C).

According to the procedures explained (see the Theoretical Framework), the following parameters are calculated: dynamic fracture toughness K_{Id}, and critical stress intensity factors K_{Jc} and K_{Ji}, as a function of testing temperature, T. From figures 11 and 12 it is evident that the applied temperatures of –70°C and –30°C have enveloped the transitional region of the mixed brittle–ductile fracture behaviour of the tested steel.

The fracture toughness dependence on the testing temperature is shown in Figs. 11 and 12, for specimen

orientations U and P, respectively. Fracture toughness calculations strictly depend on the testing conditions, and particularly on the applied temperature. The value K_{Id} is the dynamic fracture toughness, determined from linear-elastic conditions (when the 3τ criterion is fulfilled); the value K_{Ji} is the dynamic fracture toughness determined from the critical J integral value according to the procedure for assessing the onset of stable crack initiation; K_{Jc} is the fracture toughness calculated according to standard ASTM and EPRI procedures (Electric Power Research Institute, Palo Alto, CA, USA), or by linear-elastic analysis (Tada, Paris, Irwin, 1973).

Methods based on linear elastic material behaviour were applied in calculating the fracture toughness at lower temperatures, since cleavage is the dominant fracture mechanism. The applied relations of linear elastic fracture mechanics, based on quasi-static testing conditions (ASTM, EPRI, Tada et al.), give lower values for fracture toughness compared to the values derived from the impact response curve concept (see Fig. 11). At intermediate testing temperatures, close to the upper shelf fracture toughness region, the experimental procedure from the applied magnetic emission technique, for determining the onset of stable crack initiation, was applied. The determination of the characteristic time-to-fracture and the plastic component of absorbed energy have enabled the evaluation of the parameters J_{cm}^{d} and K_{Ji}. The large scattering of results is expected since other testing parameters are varied (pre-crack length, a_o, and impact speed, v_o).

Similarly to the results in Fig. 11, the fracture toughness vs. testing temperature dependence for P orientation specimens is shown in Fig. 12. As in the former case, the application of standard relations of linear-elastic fracture mechanics for quasi-static testing conditions has also resulted in lower fracture toughness values, compared to the values obtained from the impact response curve concept. Higher values for the dynamic fracture toughness are obtained at lower testing temperatures when determined by using the method for detecting stable (or unstable) crack initiation (as for ductile behaviour). Owing to this, it is assumed that values of dynamic fracture mechanics parameters of the tested high strength micro-alloyed steel should be higher than values obtained from previous and numerous static tests found in literature.

Analysis of the force–time, ME–time, and MF–time curves shows diverse fracture behaviour, from very brittle to very ductile. The material fracture toughness is largely influenced by impact speed, and in the case of ductile behaviour, the fracturing mechanism is conditioned by the strain field. The fracture toughness, as a material property, may decrease or increase, depending on the impact speed (Grabulov, 1995; Yoon et al., 1999).
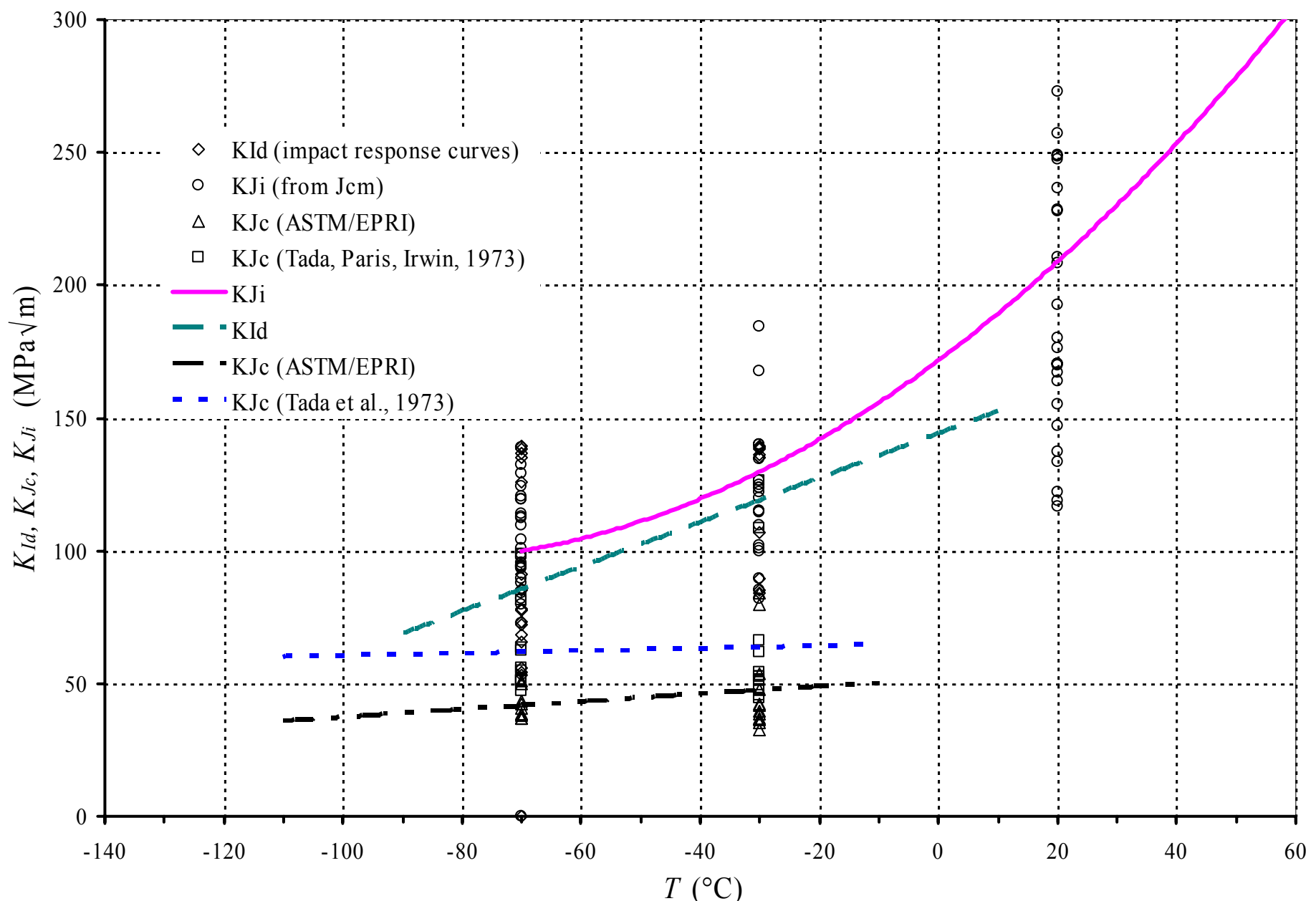

Figure 11. Fracture toughness by cleavage, ductile tearing, or by mixed mode in the transition temperature region of the tested specimens with L–S orientation (***U***).
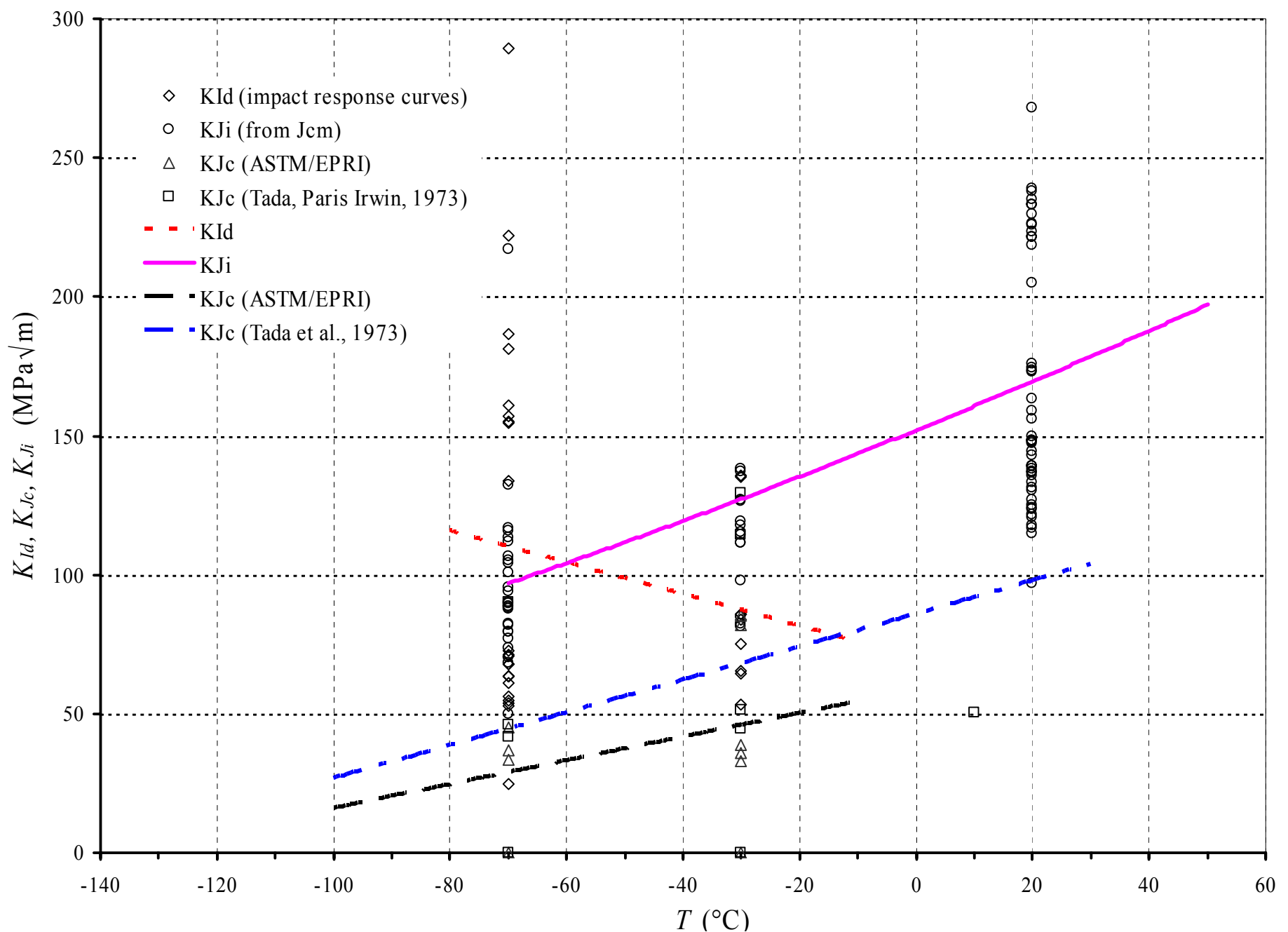
Figure 12. Fracture toughness by cleavage, ductile tearing, or by mixed mode in the transition temperature region of the tested specimens with T–S orientation (*P*).

5. CONCLUSIONS

The applied magnetic emission technique was successful in determining stable and unstable crack initiation. The tested material showed high ductility behaviour, consistent even at lower temperatures. Brittle behaviour at low temperatures is characterised by elastic material properties driven by mechanism of cleavage fracture. At room temperature conditions, the material underwent ductile tearing by mechanism of micro-void coalescence. It is very well known that all engineering materials and alloys, and particularly micro-alloyed steels contain inclusions and second-phase particles, to a greater or lesser extent (subsequent visual and microscopic examination of the fractured surfaces of many of the tested specimens revealed a relatively high concentration of inclusions). On the account of these irregularities, the material subjected to impact should experience microvoid nucleation and growth, which may be terminated at a very early stage during, e.g. tension testing (qausi-static test), by localised *internal* necking of the intervoid matrix across a sheet of microvoids (Thomason, 1990). Clearer understanding of the physical mechanisms of ductile fracture will be obtained from scanning-electron microscope (SEM) studies of the plastic flow and fracture.

Anyhow, in these situations, methods of elastic-plastic fracture mechanics are applied. The region of transition temperature was characterised by mixed fracture behaviour, both brittle and ductile. This allowed for application of specific methods of determining dynamic fracture mechanics parameters, described by existing standards (elastic-plastic fracture mechanics, ASTM/ EPRI), and also in new non-standard experimental procedures for determining these quantities (the magnetic emission technique).

The dynamic fracture mechanics properties of the tested material have been determined as a function of pre-crack length and temperature. The orientation of the texture had little influence on the critical dynamic fracture mechanics parameters for longer cracks.

Successful application of the magnetic emission technique in the instrumented Charpy testing, despite the large number of tested specimens made of the ferritic-pearlitic high strength micro-alloyed steel, may still not be considered statistical, because of the large number of factors that influence dynamic fracture. The advantages of the magnetic emission technique have been carefully exploited, enabling the determination of unstable and stable fracture development. Pure magnetic emission (ME) signal analysis proved to be sufficient for unstable crack growth, as a characteristic of the cleavage fracturing mechanism. In cases of ductile fracture, characterised by stable crack growth, analysis of the integrated magnetic emission signal (MF) was additionally needed, as well as the applied load (*F*). The procedure for analyzing the MF signal is of newer date and its physical interpretation is adopted as the quantity proportional to the intensity of external magnetic field of the tested material, in the vicinity of the developing

crack. Three testing temperatures were chosen (–70°C, –30°C, and +20°C).

At lower temperature (–70°C) and higher impact speed (5,5 m/s), the result is a very slow drop in the J integral as a function of pre-crack length, a_o. The J integral drops even slower for specimens with transversal (T–S) orientation of texture. Small values for critical dynamic J integral (J_{cm}^d), at unstable crack initiation, appear due to brittle fracture behaviour. At lower impact speeds (2,59 m/s) the J integral value also drops very slowly as a function of pre-crack length, but with a greater difference when considering texture orientation which is a logical result when lower impact speed is applied, since the orientation of texture has even greater influence at lower impact speeds. Slower rate of J integral drop for specimens of the T–S orientation confirms lesser susceptibility of pre-crack length to this orientation of texture.

At lower temperatures just prior to dominating transition effects (–30°C) and at higher impact speeds (5,5 m/s), the resulting dependence should be taken with precaution. The ductile steel shows mixed fracture behaviour, and thus large scattering of the results. Direct evaluation of J_{cm}^d by magnetic emission technique is very uncertain and so other dynamic fracture mechanics parameters are evaluated instead (K_{Id}, K_{Jc}, K_{Ji}), according to other evaluating procedures (ASTM and EPRI, or by impact response curve method, and from the dynamic resistance curve). Higher J integral values are observed for specimens of the longitudinal orientation (L–S) at lower impact speeds (2,59 m/s), if the J value for $a/W = 0,5$ is considered as the referent.

At room temperature (+20°C) and at higher impact speed (5,5 m/s) the drop rate of J integral vs. pre-crack length is even more pronounced, and the curves of texture orientation converge as a function of pre-crack length. Texture orientation seems not to influence the critical J value for larger crack lengths. Owing to the upper shelf of fracture toughness, characterised by ductile fracture, values for J_{cm}^d are much higher than in the previous cases at –70°C and –30°C. In contrast to the previous case, the J value decreases at a lower rate at lower impact speed (2,59 m/s), whilst the curves for both texture orientations converge. Also in this case, longer pre-crack lengths do not influence the critical J integral value, and the dynamic parameter J_{cm}^d is less susceptible to pre-crack length for specimens with transversal orientation of texture (T–S).

In the region of lower testing temperatures, the fracture toughness is derived from methods based on linear elastic material behaviour. Values for fracture toughness are smaller when derived from relations of linear elastic fracture mechanics, based on quasi-static testing conditions (ASTM, EPRI, Tada et al.), than the values resulting from the concept of impact response curves. At higher testing temperature, values for J_{cm}^d and also for K_{Ji} are determined from characteristic time-to-fracture and the plastic component of absorbed impact energy. The applied technique has shown to be very precise for evaluating dynamic parameters. A relatively high scatter is expected and influenced from other testing parameters (pre-crack length, a_o, and impact speed, v_o).

A newer version of the older ASTM Standard E 813 and ASTM Standard E 1152 has been replaced by a combination of the older ASTM E 399 and the newer ASTM E 1737. These versions have been also replaced by the most recent version ASTM E 1820–01, but still these standards lack in a procedure that would be widely accepted for determining dynamic fracture mechanics parameters by testing on standard fatigue pre-cracked Charpy specimens.

Future tests will show possibilities for applying the ME technique in evaluating material resistance curves on single specimens, as is already the case with other modern techniques (e.g. the potential drop method, Grabulov, 1995).

REFERENCES

[1] ASTM Standard E-399, 1986, *Standard test method for plane strain fracture toughness of metallic materials*.

[2] ASTM Standard E 813-89, 1996, *Standard test method for J_{Ic}, a measure of fracture toughness*, 1996 Annual Book of ASTM Standards. Vol. 03.01, pp. 633-647: West Conshohocken, Philadelphia.

[3] Grabulov, V., 1995, *Evaluation of resistance curve parameters using potential drop method for crack growth measurement*, doctoral thesis (in Serbian), University of Belgrade Faculty of Technology and Metallurgy

[4] Ireland, D.R., 1980, A review of the proposed standard method of test for impact testing precracked Charpy specimen of metallic materials, Proc. of the CSNI specialists meeting, Palo Alto, Dec. 1980, CA. Electric Power Research Inst. (EPRI), pp. 1/25-1/63.

[5] Kalthoff, J.F., 1985, *Concept of Impact Response Curves*, ASM Handbook, Formerly Ninth Edition, Metals Handbook, Vol.8, Mechanical Testing, ASM International 1985, Sixth printing Oct. 1997, pp. 269-271.

[6] Kalthoff, J.F., Winkler, S., 1983, Vorrichtung zur Erfassung des Rip starts bei einer Bruchmechanikprobe, Patentanmeldung P 33 34 570.8, Deutsches Patentamt, München, Sept 1983.

[7] Lenkey, G.B., 1997, Instrumented impact testing and its application in dynamic fracture mechanics tests, 7th International Summer School of Fracture Mechanics–IFMASS 7, Velika Plana, 23-27 June 1997, eds. S. Sedmak, A. Sedmak, (in Serbian), Faculty of Technology and Metallurgy, Yugoslav Welding Association, Institute GOŠA, 2000, pp. 39-48).

[8] Lenkey, G.B., 2003, Charpy impact testing and its application in fracture mechanics, Eighth Intern. Fracture Mechanics Summer School–IFMASS 8, "From Fracture Mechanics to Structural Integrity Assessment," proceedings on CD, issued by DIVK, TMF, GOŠA Institute, Belgrade, June 2003.

[9] Lenkey, G.B., Winkler, S., 1997, On the applicability of the magnetic emission technique for the determination of ductile crack initiation in impact tests, Fracture & Fatigue of Engineering Materials & Structures, Vol. 20, No.2, 1997, pp. 143-150.

[10] Radaković, Z., 2004, *Experimental determination of dynamic fracture mechanics parameters by applying the magnetic emission technique*, doctoral thesis (in Serbian), University of Belgrade, Faculty of Mechanical Engineering

[11] Rintamaa, R., 1996, *Single specimen fracture toughness determination procedure using instrumented impact tests, Evaluating Materials Properties by Dynamic Testing*, ESIS 20, Professional Engineering Publishing Ltd., pub. arm of Institution of Mechanical Engineers, Suffolk, UK, Ed. E. van Walle

[12] Server, W.L., Wullaert, R.A., Scheckerd, J.W., 1975, Verification of the EPRI dynamic fracture toughness testing procedures, ETI Technical Report TR 75-42 for EPRI.

[13] Tada, H., Paris, P.C., Irwin, G.R., 1973, *The Stress Analysis of Cracks Handbook*, Del Research Corporation, Hellertown, Pennsylvania

[14] Thomason, P.F., 1990, *Ductile Fracture of Metals*, Pergamon Press, Oxford, UK

[15] Winkler, S.R., 1988, *Magnetische Emission, Ein neues Brucherkennungsverfahren*, Fraunhofer-Institut für Werkstoffmechanik Bericht T 3/88.

[16] Winkler, S.R., 1990, Magnetic emission detection of crack initiation, Fracture Mechanics: 21st Symposium, ASTM STP 1074, J.P. Gudas, J.A. Joyce, E.M. Hackett, Eds., ASTM, Philadelphia, pp. 178-192.

[17] Yoon, J.H., Lee, B.S., Oh, Y.J., Hong, J.H., 1999, Effects of loading rate and temperature on *J–R* fracture resistance of an SA516-Gr.70 steel for nuclear piping, International Journal of Pressure Vessels and Piping, Vol. 76, pp. 663-670.

ТЕХНИКА МАГНЕТНЕ ЕМИСИЈЕ У ПРОЦЕНИ ДИНАМИЧКИХ ПАРАМЕТАРА МЕХАНИКЕ ЛОМА ДУКТИЛНОГ ЧЕЛИКА

Зоран Радаковић

Нови изазови у процени интегритета конструкција, укључујући идентификацију опуштања и продужетак радног века конструкционих челика путем квалитативног и квантитативног одређивања динамичких параметара механике лома, имају велики значај. Проблематика експерименталних истраживања у вези је са прецизним одређивањем отпорности на лом у условима динамички оптерећених конструкција, где још увек нису дефинисане стандардне процедуре у случају Шарпи епрувета са заморном прслином.

Изведено је инструментирано Шарпи испитивање употребом технике магнетне емисије (МЕ) ради одређивања особина критичне иницијације прслине код челика са изразитим дуктилним својствима. Еквивалентно крто, дуктилно и мешовито понашање лома добијено је избором температуре испитивања и брзине удара. Успешно је спроведена анализа и одговарајућа интерпретација снимљених МЕ сигнала и интегрисаних МЕ сигнала, који су употребљени за израчунавање критичног динамичког *J* интеграла у случају нестабилног или стабилног развоја прслине.